Entanglement Renyi Negativity across a Finite Temperature Transition: A Monte Carlo Study

Kai-Hsin Wu,[1,*] Tsung-Cheng Lu,[2,†] Chia-Min Chung,[3,‡] Ying-Jer Kao,[1,§] and Tarun Grover[2,∥]

[1]Department of Physics and Center of Theoretical Sciences, National Taiwan University, Taipei 10607, Taiwan
[2]Department of Physics, University of California at San Diego, La Jolla, California 92093, USA
[3]Department of Physics and Arnold Sommerfeld Center for Theoretical Physics, Ludwig-Maximilians-Universitat Munchen, Theresienstrasse 37, 80333 Munchen, Germany

(Received 5 February 2020; accepted 21 August 2020; published 30 September 2020)

Quantum entanglement is fragile to thermal fluctuations, which raises the question whether finite temperature phase transitions support long-range entanglement similar to their zero temperature counterparts. Here we use quantum Monte Carlo simulations to study the third Renyi negativity, a generalization of entanglement negativity, as a proxy of mixed-state entanglement in the 2D transverse field Ising model across its finite temperature phase transition. We find that the area-law coefficient of the Renyi negativity is singular across the transition, while its subleading constant is zero within the statistical error. This indicates that the entanglement is short-range at the critical point despite a divergent correlation length. Renyi negativity in several exactly solvable models also shows qualitative similarities to that in the 2D transverse field Ising model.

DOI: 10.1103/PhysRevLett.125.140603

Long-range correlations in a quantum system can lead to long-range quantum entanglement. For example, the entanglement in the ground state of a $1+1$D conformal field theory (CFT) for a subregion of size ℓ takes the form $S \sim c \log \ell$ [1–3], and thus is not expressible as the sum of local terms close to the entangling boundary, i.e., $S(2\ell) \neq 2S(\ell)$, underlining the long range nature of entanglement. Similarly, the entanglement of the ground state of a $2+1$D CFT for a circular bipartition of radius R is given by $S \sim R - F$, where F again captures the long-range entanglement [4–10]. At the same time, long-range correlations do not necessarily imply long-range entanglement as is evident by considering a classical Ising model at its finite temperature critical point—the entanglement is clearly zero in this system for any bipartition. A more interesting question is to consider a quantum Hamiltonian in d space dimensions at a finite temperature critical point where the system is described by the Gibbs state $\rho \propto e^{-\beta H}$, not a pure state. The critical exponents for this system are described by a d-dimensional classical field theory [11] since the imaginary time direction is finite. What is the nature of quantum entanglement across such a transition? Does there exist any universal long-distance component of entanglement at this critical point? Although enormous progress has been made in last two decades in understanding entanglement of pure quantum states, very little is understood about the entanglement of interacting many-body quantum systems in mixed states such as the Gibbs state. In this Letter, we will study a specific quantity called entanglement Renyi negativity at a finite temperature critical point for a $2+1$D lattice model using quantum Monte Carlo (QMC) simulations, and make progress on some of these qualitative questions.

Given a density matrix ρ on a bipartite Hilbert space $\mathcal{H}_A \otimes \mathcal{H}_B$, the two parties A and B are separable if and only if ρ can be expressed as a convex combination of direct product states: $\rho = \sum_i P_i \rho_i^A \otimes \rho_i^B$. There exist several measures of entanglement that quantify how much a given state deviates from a separable state. Most of these measures require optimization over all possible states in the Hilbert space, making them intractable for many-body systems [12]. However, there does exist at least a mixed state entanglement measure called entanglement negativity [13] (henceforth just "negativity" for brevity), which does not invoke any optimization. Consider a density matrix acting on the Hilbert space $\mathcal{H}_A \otimes \mathcal{H}_B$: $\rho = \sum_{A,B,A',B'} \rho_{A,B;A'B'} |A\rangle|B\rangle\langle A'|\langle B'|$, a partial transpose operation over A gives $\rho^{T_A} = \sum_{A,B,A',B'} \rho_{A,B;A'B'} |A'\rangle|B\rangle\langle A|\langle B'|$. The negativity E_N is then defined as $E_N = \log(\|\rho^{T_A}\|_1)$. Although negativity can be zero for an entangled mixed state, a nonzero negativity necessarily implies the nonzero entanglement between the two parties.

In spite of being computable without requiring any optimization, negativity is analytically tractable only in simple models such as free bosonic and fermionic systems [14–19], $1+1$D CFTs, integrable spin chains [20–23], and systems that have a tensor network representation such as commuting projector Hamiltonians [24–28]. It is thus desirable to devise a QMC scheme for large-scale simulation. However, the definition of negativity involves a matrix one norm, which impedes the construction of a QMC algorithm. Taking a cue from a somewhat similar obstacle in the evaluation of von Neumann entropy for pure states [29], one approach is to instead consider "Renyi negativity" which involves various moments of the partial transposed density matrix. Such an object was first introduced as an analytical tool to calculate negativity in the CFT [20,30], and was later implemented in a QMC simulation by the replica trick in Refs. [31,32] for a 1D spin chain and the Bose-Hubbard model. It has also been studied in the ground state of two-dimensional free lattice models [15,16].

Here we present an extensive numerical study for Renyi negativity in the 2D transverse field Ising model (TFIM) using QMC simulations. In contrast to the 1D models in Refs. [31,32], or the free models in Refs. [15,16], the 2D TFIM hosts a finite temperature transition, which allows us to pose and answer questions related to the universal mixed state entanglement across the transition.

Renyi negativity in simple models.—The Renyi negativity of index n is defined as $R_n = -\log[(\mathrm{tr}\{(\rho^{T_A})^n\})/(\mathrm{tr}\rho^n)]$. When ρ is a pure state, R_n directly relates to Renyi entanglement entropy S_n with $R_n \propto S_n$ for odd n, and $R_n \propto S_{n/2}$ for even n. R_n reduces to $-E_N$ with an analytic continuation by sending $n \to 1$ for even n [20,30].

For a large class of lattice models and field theories relevant to our discussion, Renyi negativity shares several key features with the negativity E_N. For example, for the Gibbs state corresponding to a 1D CFT, both R_n and E_N exhibit an area law with similar dependence on temperature: $E_N, R_n \sim \log(\beta)$ [21,33]. Next, consider higher dimensional solvable models studied in Refs. [18,27] that exhibit a finite-T phase transition. The key results from these models were (i) for nonlocal models (such as the spherical model), E_N is singular across the phase transition; (ii) for local models, area-law coefficient of E_N is singular across the finite temperature phase transition; (iii) for local models, after subtracting off the local terms (which includes the area-law component), negativity decays exponentially even at the critical point: $\Delta E_N \sim e^{-L/\xi_Q}$, where ξ_Q defines a "quantum correlation length" that remains finite even at the transition. The significance of the last result implies that the long-range component of negativity vanishes in the thermodynamic limit, in agreement with the conventional wisdom that these phase transitions are "classical" rather than "quantum".

We find all these features carry over to the Renyi negativity R_n, with the difference that the temperature where the partition function $Z = \mathrm{tr}(e^{-\beta H})$ becomes singular is given by nT_c where T_c is the actual critical temperature. This is because R_n involves raising the Gibbs state to the power n, and thus the effective inverse temperature for the bulk of the system is given by $n\beta$, where β is the physical inverse temperature. To illustrate these points, first consider the quantum spherical model from Ref. [27], $H = \frac{1}{2} g \sum_{i=1}^N p_i^2 - (1/2N) \sum_{i,j=1}^N x_i x_j$, where $\{x_i\}$ is subject to the spherical constraint: $\delta[(1/N) \sum_{i=1}^N x_i^2 - \frac{1}{4}]$. This model hosts a finite-T transition at a coupling g_c and temperature T_c that satisfy the equation $2\sqrt{g_c}\coth(\frac{1}{2}\beta_c\sqrt{g_c}) = 1$. We find that although the Renyi negativities for this model are continuous functions of temperature, the derivative dR_n/dT is discontinuous at a temperature nT_c, similar to the behavior of negativity E_N [34]. Since this model is nonlocal, Renyi negativities do not follow an area law, and there is no distinction between local contributions to negativity from nonlocal ones. To that end, we next briefly report the results on Renyi negativity for a local model considered in Ref. [18]: $H = \frac{1}{2}\sum_{\vec{r}} (\pi_{\vec{r}}^2 + m^2\phi_{\vec{r}}^2) + \frac{1}{2}\sum_{\langle \vec{r}, \vec{r}' \rangle} K(\phi_{\vec{r}} - \phi_{\vec{r}'})^2$, where the physical mass obeys $m = \sqrt{T - T_{n,c}}$ for $T > T_{n,c}$, and $m = \sqrt{2(T_{n,c} - T)}$ for $T < T_{n,c}$. Here $T_{n,c} = nT_c$ gives the critical temperature of the state $\rho \sim \exp\{-n\beta H\}$. This model can be considered as a mean-field description of the TFIM while taking into account Gaussian fluctuations. We find that the area-law coefficient of the Renyi negativity has a cusp singularity at a temperature $T = nT_c$ where T_c is the physical critical temperature, while the subleading, long-distance part of Renyi negativity, defined via a subtraction scheme analogous to Kitaev-Preskill/Levin-Wen construction [35,36], decays exponentially with system size, even at the critical point [34].

Renyi negativity for $2+1$D transverse field Ising model.—The models discussed above are exactly solvable, and one might wonder if the qualitative features exhibited by them may be attributed to this fact. We now turn our focus to the TFIM on a square lattice, which is known for hosting a finite-T phase transition within 2D Ising universality, and is not exactly solvable. The Hamiltonian is given by

$$H = -\sum_{\langle ij \rangle} \sigma_i^z \sigma_j^z - h_x \sum_i \sigma_i^x, \tag{1}$$

where the σ_i^z, σ_i^x are the Pauli operators at site i, and $\langle ij \rangle$ denotes all the nearest neighbor pairs on a square lattice. We impose the periodic boundary condition, and set $h_x = 2.75$. We first locate the corresponding critical inverse temperature $\beta_c = 1.0874(1)$ from a finite size scaling of the Binder ratio $B_2 = \langle M_z^4 \rangle / \langle M_z^2 \rangle^2$ calculated by the standard stochastic series expansion (SSE) simulation [34]. This result is consistent with a previous QMC study [40].

Since the Renyi negativity R_n vanishes for $n = 1, 2$, the smallest nontrivial integer is $n = 3$, which will be the focus of our QMC simulations. R_3 can be expressed as

$$R_3(A) = -\log\left(\frac{\mathrm{tr}\{(\rho^{T_A})^3\}}{\mathrm{tr}\rho^3}\right) = -\log\left(\frac{Z[A,\beta,3]}{Z[3\beta]}\right), \tag{2}$$

where $Z[A,\beta,3] = \mathrm{tr}\{[(\exp(-\beta H))^{T_A}]^3\}$ and $Z[3\beta] = \mathrm{tr}[\exp(-3\beta H)]$ are the partition functions subjected to the boundary conditions shown in Figs. 1(a) and 1(b),

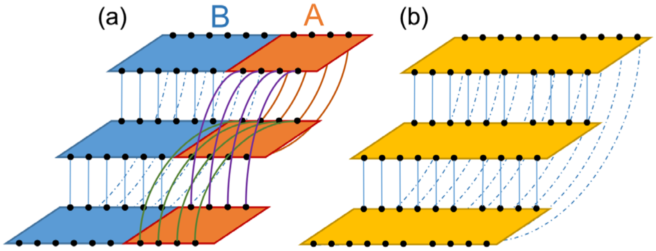

FIG. 1. Boundary conditions for different replicas in space-imaginary time for (a) $\mathrm{tr}\{(\rho^{T_A})^3\}$ and (b) $\mathrm{tr}(\rho^3)$.

respectively. Therefore, the Renyi negativity can be calculated using the SSE by numerically integrating the difference between the energy estimators for different boundary conditions:

$$R_3[\beta] = \int_0^\beta d\beta' \langle E(\beta')\rangle_{A,\beta,3} - \langle E(\beta')\rangle_{3\beta}, \tag{3}$$

where $\langle\cdots\rangle_{A,\beta,3}$ and $\langle\cdots\rangle_{3\beta}$ denote the expectation values evaluated with corresponding boundary conditions. Here, we focus on $dR_3/d\beta$ as the derivative enhances the singularity in a finite-size simulation. Since $dR_3/d\beta$ corresponds simply to the difference between the energy estimators, no thermodynamic integration is required.

Figure 2(a) shows the temperature derivative of the area-law coefficient $R_3/|\partial A|$ as a function of the temperature for different system sizes. Here $|\partial A|$ denotes the length of the boundary of region A over which partial transpose is taken. The singularity occurs at $T = 3T_c$, consistent with our expectations. To understand the precise nature of this singularity, we note that on general symmetry grounds, the leading singular contribution to the area-law coefficient of negativity $E_N/|\partial A|$ as well as its Renyi counterparts will be proportional to the energy density [18]. Therefore, $d(E_N/|\partial A|)/dT$ as well as $d(R_3/|\partial A|)/dT$ will receive a contribution proportional to the *specific heat*. For instance, in the exactly solvable model discussed above, both dE_N/dT and dR_3/dT are discontinuous across the transition, which is indeed the singular behavior of the specific heat within the mean field [34]. Returning to the 2D Ising model, we recall that the specific heat exponent $\alpha = 0$ and the correlation length exponent $\nu = 1$. Denoting the linear size of the system by L and $t = (T - T_c)/T_c$, the singular part of the specific heat in the vicinity of the critical point takes the form $c_{v,\mathrm{sing}}(L,t) \sim c_{v,\mathrm{sing}}(L,0) + f(Lt)$ where $c_{v,\mathrm{sing}}(L,0) \propto \log(L)$ and f is a universal function with the form $f(|x| \ll 1) \sim \text{constant}$, and $f(|x| \gg 1) \sim -\log(|x|)$ [41]. Note that were $\alpha \neq 0$ (e.g., in the 3D Ising model), $c_{v,\mathrm{sing}}(L,t)$ would take a different form, namely, $c_{v,\mathrm{sing}}(L,t) \sim c_{v,\mathrm{sing}}(L,0)g(Lt)$.

Figure 2(b) shows the scaling collapse of $d(R_3/|\partial A|)/dT - d(R_3/|\partial A|)/dT|_{3T_c}$ with respect to Lt, where $t = (T - 3T_c)/3T_c$, consistent with our expectation that $d(R_3/|\partial A|)/dT$ is proportional to the specific heat of

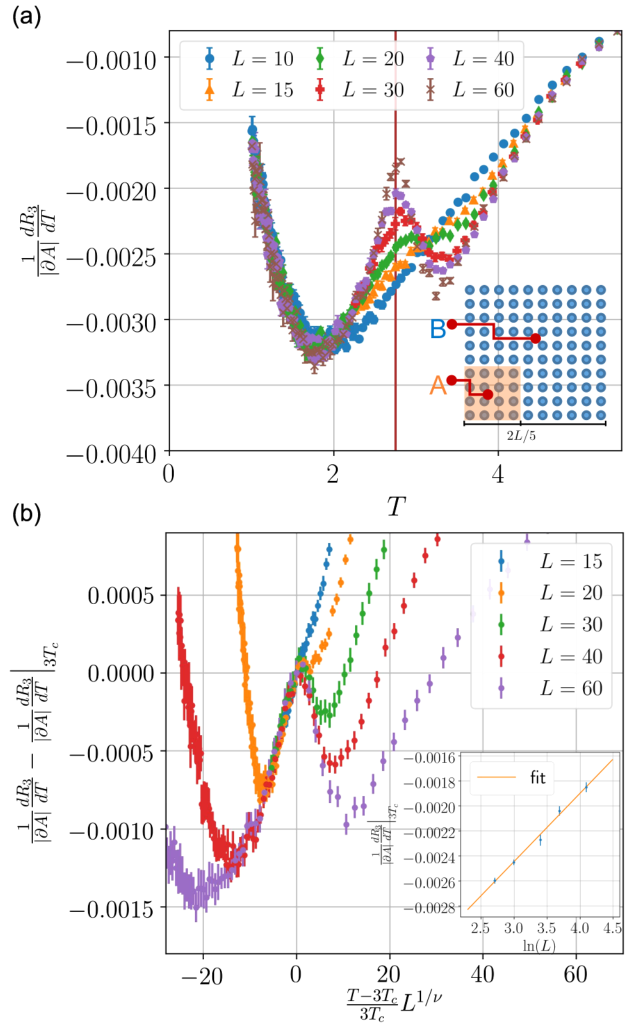

FIG. 2. (a) Temperature derivative of the area-law coefficient of the Renyi negativity across the finite temperature transition. Geometry of the bipartition is shown in the inset and the vertical line indicates the location of the transition. (b) Data collapse for Fig. 2(a). The inset shows the linear scaling of temperature derivative at the critical point with $\log(L)$.

the 2D Ising model. The inset shows the scaling right at the critical point, where we find that $d(R_3/|\partial A|)/dT \propto \log(L)$, again consistent with 2D Ising universality.

Universal long-range Renyi negativity.—Now we turn to the question of whether there is a *universal* subleading term in the Renyi negativity that reflects long-range quantum entanglement. Writing $R_3 = al - \gamma + b/l + \cdots$, where l is the size of the entangling boundary, we are interested in whether γ is nonzero. To extract γ we use a subtraction scheme introduced by Levin and Wen [36] in the context of the ground state topological order, to cancel out the short-distance (local) contributions to negativity. In particular, we construct four subregions S_1, S_2, S_3, and S_4 using combinations of four subparts marked as Ξ_1, Ξ_2, Ξ_3 and Ξ_4 (see inset of Fig. 3). The subregions S_i are defined as $S_1 \equiv \Xi_1 \cup \Xi_4$, $S_2 \equiv \Xi_1 \cup \Xi_2 \cup \Xi_4$, $S_3 \equiv \Xi_1 \cup \Xi_2 \cup \Xi_3 \cup \Xi_4$, and

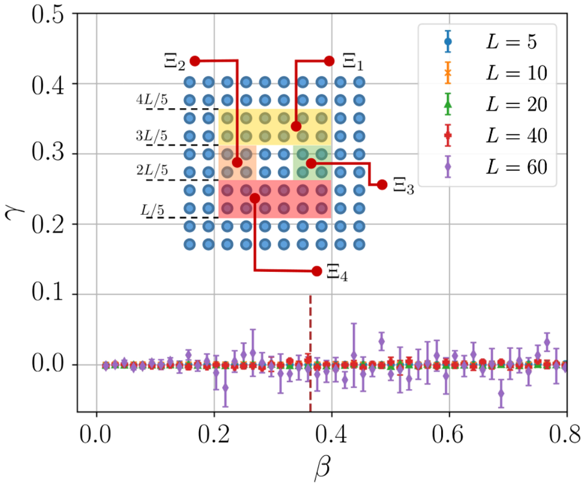

FIG. 3. The subleading contribution γ to the third Renyi negativity R_3 obtained via Levin-Wen's subtraction scheme across the critical temperature. The inset shows the four subparts Ξ_1, Ξ_2, Ξ_3, and Ξ_4 employed in the subtraction scheme (see the main text for details). The dashed vertical line shows the location of the critical point.

$S_4 \equiv \Xi_1 \cup \Xi_3 \cup \Xi_4$. The nonlocal component γ of R_3 is given by

$$\begin{aligned} \gamma &= -[R_3(S_2) - R_3(S_1) - R_3(S_3) + R_3(S_4)]/2 \\ &= -[2R_3(S_2) - R_3(S_1) - R_3(S_3)]/2, \end{aligned} \tag{4}$$

where we have used the relation $R_3(S_2) = R_3(S_4)$ arising from the symmetry of the model Hamiltonian.

The most straightforward way to compute γ is to calculate $R_3(S_i)$ separately and perform the subtraction as in Eq. (4). However, this requires three independent simulations and, the errors from each $R_3(S_i)$ will cumulate in the final subtraction. Here we develop an expanded ensemble method that allows us to calculate γ in a *single* simulation. We first write γ as the logarithm of the ratio of partition functions

$$\gamma = \frac{1}{2}\log\frac{Z_{S_2}^2}{Z_{S_1}Z_{S_3}}, \tag{5}$$

where Z_{S_i} is a shorthand notation for $Z[S_i, \beta, 3]$.

To implement our method, in addition to the conventional SSE update, we also perform sampling in an expanded ensemble of the partition functions. In particular, we allow the system to switch between different partition functions Z_{S_i} by changing the imaginary-time boundary conditions [see Fig. 1(a)]. This can be achieved by sampling the total partition function $Z_{\rm tot}$ defined as

$$Z_{\rm tot} = \sum_{i=1}^{3} Z_{S_i}, \tag{6}$$

by proposing a move from Z_{S_i} to either $Z_{S_{i+1}}$ or $Z_{S_{i-1}}$ with equal probability. The update is accepted if the spin configuration is consistent with the new boundary conditions. It is clear that these moves correspond to adding or removing only region Ξ_2 or Ξ_3, which is much smaller than S_i, so a better acceptance rate can be achieved. The ratio $Z_{S_2}^2/Z_{S_1}Z_{S_3}$ then is simply estimated by $N_{S_2}^2/N_{S_1}N_{S_3}$, where N_{S_i} is the number of samples in Z_{S_i}.

Since γ is computed in a single simulation with an enlarged ensemble, we avoid the accumulation of error in the naive postsubtraction. The new method is crucial in obtaining accurate γ, especially for the large system size $L = 60$. As the system size increases, the acceptance rates for exchanging regions Ξ_2 and Ξ_3 become smaller as more sites need to be updated. In such a case, we can further divide Ξ into several smaller subregions to add more intermediate ensembles and optimize the performance with the reweighting method [34]. The simulation typically runs with 10^8 Monte Carlo steps for smaller system sizes, and runs with around 10^9 Monte Carlo steps for larger system sizes.

Figure 3 shows the results for γ. It is essentially zero at temperatures across the transition for all the system sizes we consider, despite the fact that each individual term $R_3(S_i)$ is singular at the transition (Fig. 2). This indicates that this finite-T transition is driven purely by classical correlations and there exists no long-range entanglement at the transition, in line with our expectations based on the results from Ref. [18] and of the exactly solvable models discussed above.

Before concluding, we briefly comment on the corner contribution for Renyi negativity. For a $2+1$D CFT at zero temperature, a corner at the entangling boundary contributes a universal logarithmic term to the entanglement [15,42–45]. We expect that this logarithmic term will be replaced by a nonuniversal constant at a finite-T critical point discussed in this work if one uses (Renyi) negativity as an entanglement measure. This is due to the finite "entanglement length scale" set by the inverse temperature β (see Ref. [34] for a heuristic argument and numerical evidence in a solvable model). This is consistent with vanishing of the subleading term γ: had there been a logarithmic corner contribution, γ itself would have also diverged logarithmically under the Levin-Wen scheme.

Conclusion.—We presented the first QMC study of the Renyi negativity, a variant of negativity, across a finite-T phase transition in a nonintegrable model (2D TFIM). We found a clear signature of singularity in the area-law coefficient of bipartite Renyi negativity, and vanishing of the subleading, nonlocal part of Renyi negativity. This indicates that the long-range correlations inherent to the critical point are completely classical, and the singularity associated with quantum correlations is localized close to the boundary. To extract this subleading term, we implemented the Levin-Wen subtraction scheme using a novel Monte Carlo algorithm that automatically cancels out the leading area-law contribution in a single simulation.

We note that Ref. [46] used a linked-cluster expansion to argue that the area-law coefficient of negativity is *not* singular across the finite-T transition in the 2D TFIM. Although we only studied Renyi negativity, our results along with the results of Ref. [18] strongly suggest that the lack of any visible singularity in Ref. [46] is due to rather small system sizes accessible within the linked-cluster expansion ($L \lesssim 10$). Even for the Renyi negativity, singularity at the critical point would not be visible at such sizes.

We also extended the analytical results on the negativity of exactly solvable models to the Renyi negativity, and found that they share essentially all qualitative features close to a finite-T transition. In particular, while the area-law coefficient is singular, the subleading component γ vanishes exponentially with the system size. We are unable to do similar scaling analysis for the 2D TFIM because the Monte Carlo sampling error in γ increases rapidly when increasing the system size while the mean value of γ is close to zero.

The vanishing of the nonlocal component of Renyi negativity suggests that the Gibbs state is separable up to short-distance quantum correlations. Therefore, we expect that there exists a minimally entangled typical thermal state (METTS) decomposition [47] of the Gibbs state both near and at the finite temperature transition: $\rho = \sum_i p_i |\psi_i\rangle\langle\psi_i|$ where each pure state $|\psi_i\rangle$ is short-range entangled. Another promising future direction would be to study the Renyi negativity in 4D toric code, which is argued to host a finite temperature transition from a topological ordered phase to a topologically trivial Gibbs state [48], using a similar QMC scheme.

We thank Dan Arovas and John McGreevy for helpful discussions. This work was supported by Ministry of Science and Technology (MOST) of Taiwan under Grants No. 108-2112-M-002-020-MY3 and No. 107-2112-M-002-016-MY3, and partly supported by National Center of Theoretical Science (NCTS) of Taiwan with the Young Scholar-fellowship to K.-H. W. We are grateful to the National Center for High-performance Computing for computer time and facilities. T. G. is supported by an Alfred P. Sloan Research Fellowship, National Science Foundation under Grant No. DMR-1752417, and the University of California's Multicampus Research Programs and Initiatives (MRP-19-601445).

[*]kaihsinwu@gmail.com
[†]tsl015@ucsd.edu
[‡]chiaminchung@gmail.com
[§]yjkao@phys.ntu.edu.tw
[‖]tagrover@ucsd.edu

[1] C. Callan and F. Wilczek, Phys. Lett. B **333**, 55 (1994).
[2] C. Holzhey, F. Larsen, and F. Wilczek, Nucl. Phys. **B424**, 443 (1994).
[3] P. Calabrese and J. Cardy, J. Stat. Mech. (2004) P06002.
[4] R. C. Myers and A. Sinha, Phys. Rev. D **82**, 046006 (2010).
[5] R. C. Myers and A. Sinha, J. High Energy Phys. 01 (2011) 125.
[6] H. Casini, M. Huerta, and R. C. Myers, J. High Energy Phys. 05 (2011) 36.
[7] H. Casini and M. Huerta, Phys. Rev. D **85**, 125016 (2012).
[8] H. Casini, M. Huerta, R. C. Myers, and A. Yale, J. High Energy Phys. 10 (2015) 3.
[9] D. L. Jafferis, I. R. Klebanov, S. S. Pufu, and B. R. Safdi, J. High Energy Phys. 06 (2011) 102.
[10] I. R. Klebanov, S. S. Pufu, and B. R. Safdi, J. High Energy Phys. 10 (2011) 038.
[11] S. Sachdev, *Quantum Phase Transitions* (Cambridge University Press, Cambridge, England, 2011).
[12] R. Horodecki, P. Horodecki, M. Horodecki, and K. Horodecki, Rev. Mod. Phys. **81**, 865 (2009).
[13] G. Vidal and R. F. Werner, Phys. Rev. A **65**, 032314 (2002).
[14] K. Audenaert, J. Eisert, M. B. Plenio, and R. F. Werner, Phys. Rev. A **66**, 042327 (2002).
[15] C. D. Nobili, A. Coser, and E. Tonni, J. Stat. Mech. (2016) 083102.
[16] V. Eisler and Z. Zimborás, Phys. Rev. B **93**, 115148 (2016).
[17] H. Shapourian, K. Shiozaki, and S. Ryu, Phys. Rev. B **95**, 165101 (2017).
[18] T.-C. Lu and T. Grover, arXiv:1907.01569.
[19] H. Shapourian and S. Ryu, J. Stat. Mech. (2019) 043106.
[20] P. Calabrese, J. Cardy, and E. Tonni, Phys. Rev. Lett. **109**, 130502 (2012).
[21] P. Calabrese, J. Cardy, and E. Tonni, J. Phys. A **48**, 015006 (2015).
[22] H. Wichterich, J. Molina-Vilaplana, and S. Bose, Phys. Rev. A **80**, 010304(R) (2009).
[23] P. Ruggiero, V. Alba, and P. Calabrese, Phys. Rev. B **94**, 035152 (2016).
[24] Y. A. Lee and G. Vidal, Phys. Rev. A **88**, 042318 (2013).
[25] C. Castelnovo, Phys. Rev. A **88**, 042319 (2013).
[26] O. Hart and C. Castelnovo, Phys. Rev. B **97**, 144410 (2018).
[27] T.-C. Lu and T. Grover, Phys. Rev. B **99**, 075157 (2019).
[28] J. Gray, arXiv:1809.01685.
[29] M. B. Hastings, I. González, A. B. Kallin, and R. G. Melko, Phys. Rev. Lett. **104**, 157201 (2010).
[30] P. Calabrese, J. Cardy, and E. Tonni, J. Stat. Mech. (2013) P02008.
[31] V. Alba, J. Stat. Mech. (2013) P05013.
[32] C.-M. Chung, V. Alba, L. Bonnes, P. Chen, and A. M. Läuchli, Phys. Rev. B **90**, 064401 (2014).
[33] V. Eisler and Z. Zimborás, New J. Phys. **16**, 123020 (2014).
[34] See Supplemental Material at http://link.aps.org/supplemental/10.1103/PhysRevLett.125.140603 for additional results and details about the Renyi negativity and expanded ensemble method, Renyi negativity in qunautm spherical model, Renyi negativity at gaussian fixed point, and corner contribution of Renyi-negativity, which includes Refs. [18,21,27,33,35–39].
[35] A. Kitaev and J. Preskill, Phys. Rev. Lett. **96**, 110404 (2006).
[36] M. Levin and X.-G. Wen, Phys. Rev. Lett. **96**, 110405 (2006).

[37] A. Serafini, *Quantum Continuous Variables: A Primer of Theoretical Methods* (CRC Press, Boca Raton, 2017).
[38] Y. Iba, Int. J. Mod. Phys. C **12**, 623 (2001).
[39] J. Helmes, doctoral thesis, Universität zu Köln, 2017.
[40] S. Hesselmann and S. Wessel, Phys. Rev. B **93**, 155157 (2016).
[41] A. E. Ferdinand and M. E. Fisher, Phys. Rev. **185**, 832 (1969).
[42] H. Casini and M. Huerta, Nucl. Phys. **B764**, 183 (2007).
[43] H. Casini, M. Huerta, and L. Leitao, Nucl. Phys. **B814**, 594 (2009).
[44] E. M. Stoudenmire, P. Gustainis, R. Johal, S. Wessel, and R. G. Melko, Phys. Rev. B **90**, 235106 (2014).
[45] A. B. Kallin, E. M. Stoudenmire, P. Fendley, R. R. P. Singh, and R. G. Melko, J. Stat. Mech. (2014) P06009.
[46] N. E. Sherman, T. Devakul, M. B. Hastings, and R. R. P. Singh, Phys. Rev. E **93**, 022128 (2016).
[47] E. M. Stoudenmire and S. R. White, New J. Phys. **12**, 055026 (2010).
[48] E. Dennis, A. Kitaev, A. Landahl, and J. Preskill, J. Math. Phys. (N.Y.) **43**, 4452 (2002).